Towards Quantum Advantage in Lattice Gauge Theory Calculations

George Siopsis

Department of Physics and Astronomy
The University of Tennessee
Knoxville, TN 37996-1200, USA

January 14, 2025

THE UNIVERSITY OF
TENNESSEE
KNOXVILLE

Outline

- Motivation
- Quantum Computing with Fields
- Scalar Quantum Field Theory (QFT)
- SU(2) Lattice Gauge Theory (LGT)
- Conclusion

K Marshall, R Pooser, GS, C Weedbrook, Physical Review A 92, 063825 (2015).
CW Bauer, *et al.*, Physical Review X Quantum 4, 027001 (2023).
RG Jha, F Ringer, GS, S Thompson, Physical Review A 109, 052412 (2024).
RA Briceño, *et al.*, Physical Review Research 6, 043065 (2024).
V Ale, NM Bauer, RG Jha, F Ringer, GS, arXiv:2410.14580.

Motivation

LGTs: Core to understanding the Standard Model, including QCD.

- Challenges in Classical LGT:
  - Real-time dynamics.
  - Finite-density and thermal systems.
  - Exponential computational cost.
  - Truncation: Finite-dimensional representation of continuous gauge groups.
  - Sign Problem: Severe cancellations in MC integration.
  - High-Dimensional Systems: Inefficiency of tensor network methods beyond 2D.
- Quantum Computing Offers:
  - Direct simulation of Hamiltonian evolution.
  - Solving the sign problem in MC methods.
- Quantum Advantage in Perspective:
  - Objective: Address computational bottlenecks in nonperturbative QFTs.
  - Ultimate Goal: Real-time, FT simulations for QCD in 3+1 d.

Continuous-Variable Quantum Computing

- Qumodes:
  - Represented as quantum harmonic oscillators.
  - Infinite-dimensional Hilbert space ideal for gauge fields.
- Advantages:
  - Avoids truncation of continuous symmetries.
  - Efficient parameterization of Hamiltonians.
- Photonic Quantum Processors
  - Continuous-Variable Framework: Encodes information in optical quadratures Q, P.
  - Scalable Architectures: Generation of cluster states with thousands of qumodes.

- Quantum fields are fundamental constituents of the physical world, describing quantum many-body systems of matter at all energy scales, as well as electromagnetic and gravitational radiation. Quantum-field engineering has enabled unprecedented measurement sensitivities, epitomized by the use of squeezed light to lower the noise floor of the Laser Interferometer Gravitational-wave Observatory (LIGO) below the shot noise limit.
- The encoding of quantum information in continuous-variable (CV) quantum fields, a.k.a. qumodes (in lieu of discrete-variable qubits), has enabled multipartite entanglement over millions of qumodes. This scale, unparalleled in any qubit architecture, defines new horizons and paradigms for quantum computing, quantum communication and quantum sensing. Nanophotonic integrated devices based on qumodes have the potential to define future quantum technology by surpassing the performance of qubit-based NISQ computing devices.
- A natural implementation of qumodes uses quantum light, which also lends itself to sensing and communication. The coming of age of low-loss, high-nonlinearity integrated optics paves the way for implementing large-scale, fault-tolerant quantum computing and communication devices on chip, at room temperature, and within a few years.

CV QC

Continuous-variable (CV) quantum computation (QC) and is an alternative to more traditional qubit methods. The fundamental idea is to not consider a system of two-state systems (qubits) or d-state systems (qudits) but to harness the power of the infinite-dimensional representation in terms of bosonic fields. In addition to access to enhanced Hilbert space, a CV quantum computer based can make use of photonic elements to build states that are better suited for maintaining coherence and quantum error correction.

- A qumode is an infinite-dimensional harmonic oscillator of quadratures (q, p),

$$\hat{q} = \frac{1}{\sqrt{2}}\left(\hat{a}^\dagger + \hat{a}\right) \ , \ \ \hat{p} = \frac{i}{\sqrt{2}}\left(\hat{a}^\dagger - \hat{a}\right)$$

  where $\hat{a}$ and $\hat{a}^\dagger$ are bosonic creation and annihilation operators with $[\hat{a}, \hat{a}^\dagger] = 1$.

Single-qumode gates

Squeezing is implemented by

$$\hat{S}(r) = e^{\frac{r}{2}\left(\hat{a}^{\dagger 2} - \hat{a}^2\right)}, \quad \hat{S}^\dagger(r)\hat{q}\hat{S}(r) = e^{-r}\hat{q}\,, \quad \hat{S}^\dagger(r)\hat{p}\hat{S}(r) = e^{r}\hat{p}$$

Displacement gate equipped with a real parameter x,

$$e^{-i\hat{p}x} = D(x/\sqrt{2}) = e^{\frac{x}{\sqrt{2}}\left(\hat{a}^\dagger - \hat{a}\right)}, \quad \hat{q} \to \hat{q} + x\,, \quad \hat{p} \to \hat{p}$$

Rotation gate with $\theta \in \mathbb{R}$

$$\hat{R}(\theta) = e^{i\hat{N}\theta}\,, \quad \hat{N} = \frac{1}{2}\left(\hat{q}^2 + \hat{p}^2\right)\,, \quad \begin{pmatrix}\hat{q}\\ \hat{p}\end{pmatrix} \to \begin{pmatrix}\cos\theta & -\sin\theta\\ \sin\theta & \cos\theta\end{pmatrix}\begin{pmatrix}\hat{q}\\ \hat{p}\end{pmatrix}$$

Quadratic phase gate,

$$\hat{P}(s) = e^{is\hat{q}^2/2}, \quad \hat{P}^\dagger(s)\hat{q}\hat{P}(s) = \hat{q}\,, \quad \hat{P}^\dagger(s)\hat{p}\hat{P}(s) = \hat{p} + s\hat{q}$$

Two-qumode gates

Beam splitter, $\theta \in \mathbb{R}$,

$$\hat{\mathrm{BS}}_{i,j}(\theta) = e^{\theta(\hat{a}_i \hat{a}_j^\dagger - \hat{a}_i^\dagger \hat{a}_j)}, \quad \begin{pmatrix} \hat{q}_i/\hat{p}_i \\ \hat{q}_j/\hat{p}_j \end{pmatrix} \to \begin{pmatrix} \cos\theta & -\sin\theta \\ \sin\theta & \cos\theta \end{pmatrix} \begin{pmatrix} \hat{q}_i/\hat{p}_i \\ \hat{q}_j/\hat{p}_j \end{pmatrix}$$

CX gate,

$$\hat{\mathrm{CX}}_{i,j}(s) = e^{-is\hat{q}_i\hat{p}_j}, \quad \begin{aligned} \hat{q}_i &\to \hat{q}_i\ , \quad \hat{p}_i \to p_i - s\hat{p}_j \\ \hat{p}_j &\to \hat{p}_j\ , \quad \hat{q}_j \to \hat{q}_j + s\hat{q}_i \end{aligned}$$

can be decomposed in beam splitters and single-mode squeezers.

- Readily available set of Gaussian operations, corresponding to Hamiltonians of first and second powers of $\hat{q}$ and $\hat{p}$.

Non-Gaussian Gate

To achieve universal CV QC, one needs a non-Gaussian element. Simplest is the cubic phase gate

$$\phi(s) = e^{i\frac{s}{3}\hat{q}^3}$$

For deterministic implementation for small s, we first engineer the resource state $|s\rangle = \phi(s)\,|p = 0\rangle$. The implement the circuit

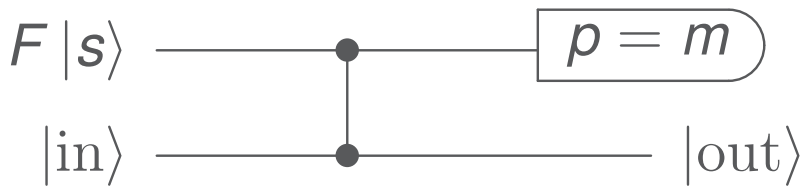

We obtain $|\mathrm{out}\rangle = e^{ism\hat{q}^2} e^{ism^2\hat{q}}\phi(s)\,|\mathrm{in}\rangle$.
After applying the Gaussian gates $e^{-ism\hat{q}^2}$, $e^{-ism^2\hat{q}}$, we obtain the desired state $\phi(s)\,|\mathrm{in}\rangle$.

[P Marek, R Filip, A Furusawa, PRA **84**, 053802 (2011)]

The resource state $|s\rangle$ can be engineered by decomposing $\phi(s) \approx 1 + i\frac{s}{3}\hat{q}^3$ into 3 linear factors

[K Marshall, R Pooser, GS, C Weedbrook, PRA **91**, 032321 (2015)]

or by more sophisticated quantum circuits using machine learning

[S Abel, M Spannowsky, S Williams, PRA **110**, 012607 (2024)]

Other non-Gaussian gates can be implemented using the cubic phase gate and the Baker–Campbell–Hausdorff formula

$$e^A e^B e^{-A} e^{-B} = e^{[A,B]+\ldots}$$

for small A, B. Example:

$$e^{-\frac{i}{2}\delta t(u_1^2 P_1^2 + P_1^2 u_1^2)} \approx e^{\frac{i}{3}\sqrt{\delta t}u_1^3} e^{\frac{i}{3}\sqrt{\delta t}P_1^3} e^{-\frac{i}{3}\sqrt{\delta t}u_1^3} e^{-\frac{i}{3}\sqrt{\delta t}P_1^3}$$

for small s. The gate $e^{\frac{i}{3}s\hat{p}^3}$ is obtained by applying the Fourier transform to $\phi(s)$, with

$$F = e^{i\frac{\pi}{2}N}, \quad N = \frac{1}{2}(\hat{p}^2 + \hat{q}^2)$$

Linear Gate

To implement $\mathcal{U} = 1 + \gamma\hat{q}$ on an arbitrary state $|\psi\rangle = \int dq\, \psi(q)\, |q\rangle$,

- first prepare a weak coherent state (resource mode)

$$|\alpha\rangle_R = D(\alpha)\,|0\rangle_R \ , \quad D(\alpha) = \exp(\alpha\hat{a}_R^\dagger - \alpha^*\hat{a}_R) \ , \quad \alpha_1 \in \mathbb{R}$$

- then interact our state of interest with the coherent state under two-mode operator $U_2(\beta) = \exp[(\beta\hat{a}_R^\dagger - \beta^*\hat{a}_R)\hat{q}]$, $\beta = \gamma\alpha$
  - quantum non-demolition (QND) gate
  - requires two offline squeezed ancilla states

  [Yoshikawa, Miwa, Huck, Andersen, van Loock, Furusawa, PRL **101**, 250501 (2008)]

- arrive at the state

$$|\Psi\rangle = \int dq\, \psi(q) U_2(\beta) D_R(\alpha)\, |q\rangle\, |0\rangle_R = \int dq\, \psi(q)\, |q\rangle\, |\alpha\mathcal{U}\rangle_R$$

Linear Gate cont..

Apply a non-demolition measurement on the resource mode projecting it onto the space orthogonal to $|0\rangle$, i.e. ($P_{\bar{0}} = \hat{\mathbb{1}} - |0\rangle\langle 0|$),

$$P_{\bar{0}} |\alpha\mathcal{U}\rangle_R = e^{-|\alpha\mathcal{U}|^2} \sum_{k=1}^{\infty} \frac{1}{\sqrt{k!}} \alpha^k \mathcal{U}^k |k\rangle_R \approx \alpha\mathcal{U} |1\rangle_R$$

Error in approximation negligible for small q, significant for large q.

$$|\Psi\rangle \to \int dq\, \psi(q)\mathcal{U} |q\rangle |1\rangle_R ,$$

$\hookrightarrow$ *Repeat-until-success method:* Measurement may fail, however if it does, simply discard the mode and attempt the procedure again.
$\hookrightarrow$ Need $M \sim \mathcal{O}(1/p)$ steps, where p is the probability of subtracting a single photon.

Detector imperfections

- Efficiency $\eta < 1$
  (have successfully subtracted a photon but are unaware of this fact; attempt further photon subtractions increasing the power on the factor $\mathcal{U}_l^{k>1}$ in an undesired manner)
- dark count $\nu > 0$
  (we believe we have subtracted a photon when we have not; one of the $\mathcal{U}_l$ operators is replaced by the identity operation)

Quantum Error Correction

Theory of quantum error correction (QEC) codes for systems described by DV (qubits) is advanced.

- Not so for CV systems.
  - Gaussian errors – need non-Gaussian elements to correct.

    [Niset, Fiurasek, and Cerf, PRL **102**, 120501 (2009)]
  - Non-Gaussian errors – need only Gaussian elements to correct.

    [van Loock, arXiv:0811.3616 [quant-ph]; Ralph, PRA **84**, 022339 (2011)]
  - In addition to decoherence, errors are due to having to replace ideal states (eigenstates of quadrature operators $\hat{q}$ and $\hat{p}$) used in several algorithms with *squeezed* states, or encode information on *cat* states (superpositions of coherent states, which do not form an orthonormal set).

GKP encoding

[Gottesman, Kitaev, and Preskill, PRA **64**, 012310 (2001)]

- One logical qubit per qumode – computational basis $|x\rangle_L$ ($x = 0, 1$) formed as an evenly spaced comb of δ-functions separated by $2\sqrt{\pi}$ with the two states offset by $\sqrt{\pi}$ from each other, $|x\rangle_L \propto \sum_{n=-\infty}^{\infty} |q = (2n + x)\sqrt{\pi}\rangle$.
- Physically, eigenstates of $\hat{q}$ are replaced by sharp Gaussians enclosed by a large Gaussian envelope.
- Protected against random shifts in the quadrature variables.
- Can be used in *fault-tolerant* measurement-based QC, if squeezing is above the threshold value of 20.5 dB.

  [Menicucci, PRL **112**, 120504 (2014)]

  - A state with over a million modes has been demonstrated.

  [Yoshikawa, Yokoyama, Kaji, Sornphiphatphong, Shiozawa, Makino, and Furusawa, APL Photonics 1, 060801 (2016)]

  - 20 dB squeezing has been achieved.

Cat states

superpositions of coherent states

[Mirrahimi, Leghtas, Albert, Touzard, Schoelkopf, Jiang, and Devoret, New J. Phys. **16**, 045014 (2014)]

- Two-legged cat: $|x\rangle_L \propto |\beta\rangle + (-)^x|-\beta\rangle$, $(x = 0, 1)$.
  - ▶ Quasi-orthogonal, ${}_L\langle 0|1\rangle_L \sim e^{-|\beta|^2} \to 0$, as $\beta \to \infty$.
  - ▶ Evolution through two-photon driven dissipative process

$$\frac{d\rho}{dt} = \frac{\kappa}{2}[\beta^2\hat{a}^{\dagger 2} - \text{h.c.}, \rho] + \kappa\mathcal{D}[\hat{a}^2]\rho$$

implemented within circuit QED.

- ▶ Obey Knill-Laflamme conditions

[Knill and Laflamme, PRA **55**, 900 (1997)]

- ▶ Protected against dephasing, but not single-photon loss errors.

- Four-legged cat: $|x\rangle_L \propto |\beta\rangle + (-)^x|i\beta\rangle + |-\beta\rangle + (-)^x|-i\beta\rangle$.
  ▶ Protected against both dephasing and single-photon loss errors.
  ▶ Protection against dephasing to *unlimited* order as $\beta \to \infty$.
- $2L$-legged cat: protected against $L-1$ photon losses.
- Generalization: Use photon number eigenstates $|n\rangle$ for orthonormal basis.

  [Michael, Silveri, Brierley, Albert, Salmilehto, Jiang, Girvin, PRX **6**, 031006 (2016)]

  ▶ Find an orthonormal set to encode a logical qubit for a given master equation and set of errors, by checking the Knill-Laflamme conditions.
  ▶ Example: $|0\rangle_L = \frac{1}{2}(|0\rangle + \sqrt{3}|6\rangle)$, $|1\rangle_L = \frac{1}{2}(\sqrt{3}|3\rangle + |9\rangle)$ are protected against dephasing and single as well as double photon loss.

Scalar Field Theory

One dimension for simplicity – can be generalized.
Discretization: Choose units in which lattice spacing $a = 1$;
$x = 0, 1, \ldots, L-1$, $L \gg 1$.
Scalar field $\hat{\phi}$, conjugate $\hat{\pi}$; they obey $[\hat{\phi}_x, \hat{\pi}_{x'}] = i\delta_{xx'}$.
Periodic boundary conditions: $\hat{\phi}_L = \hat{\phi}_0$.
Free Hamiltonian

$$\hat{H}_0 = \frac{1}{2}\sum_{x=0}^{L-1}\left[\hat{\pi}_x^2 + (\hat{\phi}_x - \hat{\phi}_{x+1})^2 + m^2\hat{\phi}_x^2\right]$$

Write $\hat{H}_0 = \frac{1}{2}\boldsymbol{\pi}^T\boldsymbol{\pi} + \frac{1}{2}\boldsymbol{\phi}^T\boldsymbol{V}\boldsymbol{\phi}$. Eigenvalues and eigenvectors of $\boldsymbol{V}$,

$$\omega_k = m^2 + 4\sin^2\frac{\pi k}{L}\ , \quad e_x^k = \frac{1}{\sqrt{L}}e^{2\pi ikx/L}\ , \quad k = 0, \ldots, L-1$$

Massless case: $\boldsymbol{V}$ has zero mode. Shift m by $\sim 1/L$ to avoid problems.

Initial state

Define $\hat{A}_x = \frac{1}{\sqrt{2}}(\hat{\phi}_x + i\hat{\pi}_x)$. Commutation relations: $[\hat{A}_x, \hat{A}^\dagger_{x'}] = \delta_{xx'}$.
Define vacuum by $\hat{A}_x|0\rangle = 0$ (product of vacuum fields).
Need ground state of $\hat{H}_0$.

- Diagonalize $\hat{H}_0$: Define $\hat{a}_k = \sqrt{\frac{\omega_k}{2}}(\boldsymbol{e}^\dagger \phi)_k + \frac{i}{\sqrt{2\omega_k}}(\boldsymbol{e}^\dagger \pi)_k$.
  They obey $[a_k, a^\dagger_{k'}] = \delta_{kk'}$. After normal ordering,

$$\hat{H}_0 = \sum_{k=0}^{N-1} \omega_k \hat{a}^\dagger_k \hat{a}_k$$

  Ground state: $\hat{a}_k|\Omega\rangle = 0$.
- Let $\hat{a}_k = \hat{U}^\dagger \hat{A}_k \hat{U}$, where $\hat{U}$ is Gaussian unitary ($\sim \mathcal{O}(N^2)$ gates).
  Ground state: $|\Omega\rangle = \hat{U}^\dagger|0\rangle$.
  Similarly for excited states: $\hat{a}^\dagger_k|\Omega\rangle = \hat{U}^\dagger \hat{A}^\dagger_k|0\rangle$.

Quantum computation

Initial state: Single particle wavepacket: $\sum_k f_k \hat{a}_k^\dagger |\Omega\rangle$
(f_k strongly peaked at $k = k_0$)
n-particle wavepackets ($n \geq 2$) similar.
Calculate scattering amplitude with quartic interaction and counter term, respectively,

$$\hat{H}_{\text{int}} = \frac{\lambda}{4!} \sum_x \hat{\phi}_x^4 \,, \quad H_{\text{c.t.}} = \frac{\delta_m}{2} \sum_x \hat{\phi}_x^2$$

Time evolution implemented via successive unitaries

$$e^{i\delta t \hat{H}_{\text{int}}} e^{i\delta t \hat{H}_{\text{c.t.}}} e^{i\delta t \hat{H}_0}$$

Coupling constants are turned on and off adiabatically.
Unitaries $e^{i\delta t \hat{H}_0}$ and $e^{i\delta t \hat{H}_{\text{c.t.}}}$ are Gaussian.
Remaining unitary is implemented through quartic phase gates,

$$e^{i\delta t \hat{H}_{\text{int}}} = \prod_x e^{i\delta t \frac{\lambda}{4!} \hat{\phi}_x^4}$$

Final measurement

Final state: $|\mathrm{out}\rangle = \hat{a}^\dagger_{k_1}\hat{a}^\dagger_{k_2}\cdots|\Omega\rangle = \hat{U}^\dagger\hat{A}^\dagger_{k_1}\hat{A}^\dagger_{k_2}\cdots|0\rangle$
Uncompute by applying the Gaussian unitary U, and then measure number of photons in each mode.

- need photon-number-resolving detectors with high efficiency.
  - Polynomial growth of complexity (also with qubits), to be compared with exponential growth in classical lattice computations.
  - Feasible with current linear optical technology.

Toward Nuclear Physics

CW Bauer, *et al.*, PRX Quantum 4, 027001 (2023).
RG Jha, F Ringer, GS, S Thompson, PRA 109, 052412 (2024).

Nonlinear σ models share several features with gauge theories.

- An important application of these models is in the low-energy dynamics of pions described by an effective chiral Lagrangian density given schematically by $\mathcal{L} = \frac{1}{4}\mathrm{Tr}[\partial_\mu U \partial^\mu U^\dagger]$, where U is an isospin $SU(2)$ matrix.
- It has a global $SU(2)_L \times SU(2)_R$ symmetry which coincides with the $O(4)$ symmetry of the sigma model. This is clearly seen if we parametrize the isospin matrix as $U = u_0 + i\vec{u}\cdot\vec{\sigma}$, where σ_i are Pauli matrices, and $\boldsymbol{u} \equiv u_a n^a = u_0^2 + \vec{u}^2 = 1$.
- Define angular momenta $J_{ab} = -i(u_a \frac{\partial}{\partial u_b} - u_b \frac{\partial}{\partial u_a})$.
- The Hamiltonian discretized on a spatial lattice:

$$H = \frac{1}{2g^2}\sum_{a,b} J_{ab}^2 - g^2 \sum_{\langle x,x'\rangle} u_a(x) u^a(x')$$

- The potential is bi-linear in u_a that act as coordinates.

Non-Abelian Gauge Theories

A gauge theory with a local $SU(2)$ symmetry can also be formulated in terms of matrices on the lattice.

- The matrices $U = u_0 \mathbb{I} + i\vec{u} \cdot \vec{\sigma}$ reside on the links along which one also defines angular momenta $J_{ab} = -i(u_a \frac{\partial}{\partial u_b} - u_b \frac{\partial}{\partial u_a})$.
- The Hamiltonian can be written as

$$H = \frac{1}{2g^2} \sum_{\text{links}} J_{ab}^2 - \frac{g^2}{2} \sum_{\text{plaquettes}} \text{Tr}[U(1)U(2)U(3)U(4)]$$

  with the Wilson loop over a plaquette in the second term.
- Expressed in terms of 4d vectors $n_a(i)$ with $i = 1, 2, 3, 4$, we obtain a quadri-linear expression for a plaquette:

$$u^a(1)u_a(2)\, u^b(3)u_b(4) - u^a(1)u_a(3)\, u^b(2)u_b(4) + u^a(1)u_a(4)\, u^b(2)u_b(3)$$
$$+\epsilon^{abcd} u_a(1)u_b(2)u_c(3)u_d(4)$$

- The states obey the constraint $\epsilon^{abcd} J_{ab} J_{cd} \left|\Psi\right\rangle = 0$. Additionally, the system obeys Gauss's Law which further constrains the Hilbert space to the gauge singlet sector.

Single Plaquette

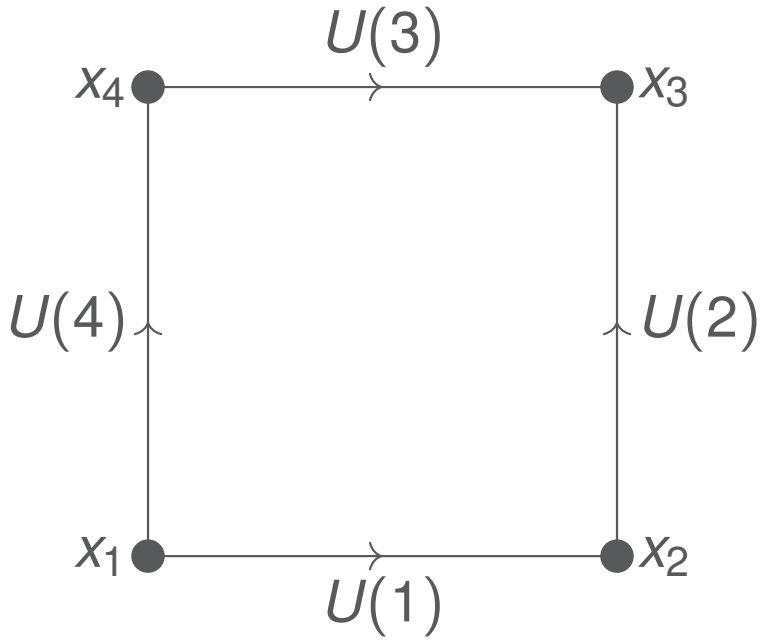

A single SU(2) plaquette with links $U(1), U(2), U(3), U(4)$.

Hamiltonian: $H = g^2(H_E + H_M)$, electric and magnetic parts,

$$H_E = \frac{1}{2}\sum J_{ab}^2 \ , \ H_M = \lambda(1 - W[C])$$

Wilson loop $W[C] = \frac{1}{2}\mathrm{Tr}[U(1)U(2)U^\dagger(3)U^\dagger(4)]$, $\lambda = \frac{4}{g^4}$.

- Continuum limit as $\lambda \to \infty$.

Analytic solutions in terms of Mathieu functions.

Results for Single Plaquette

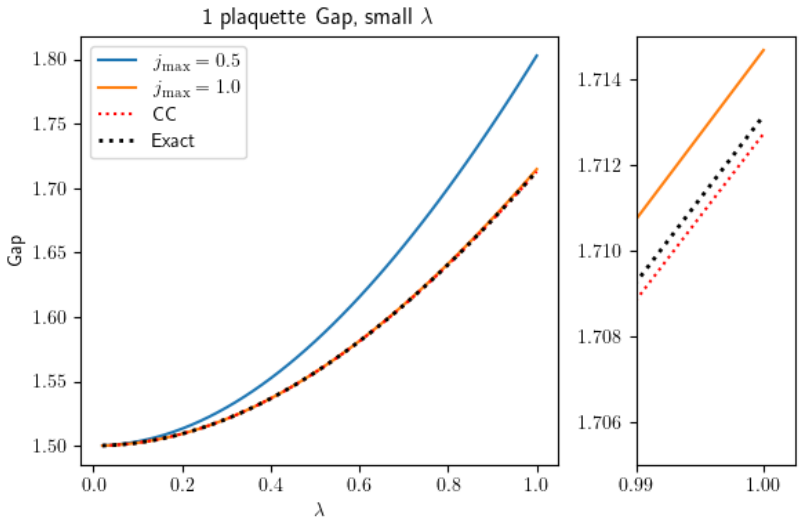

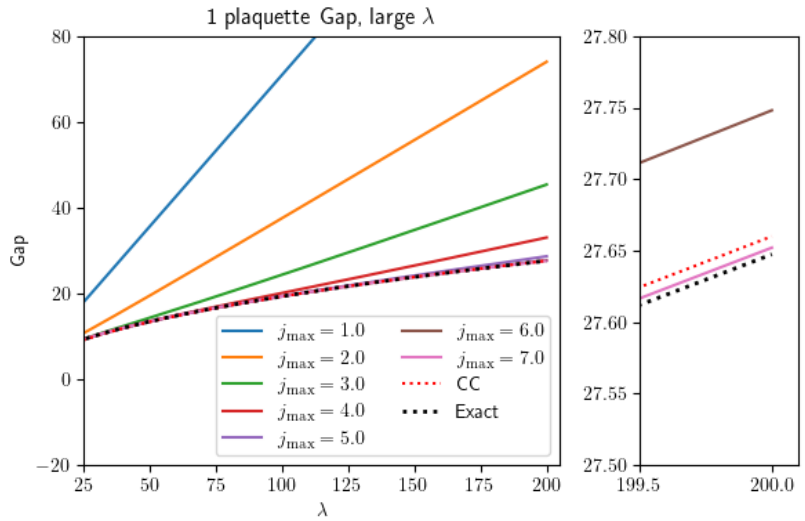

Trial wavefunctions

$$\psi_0(\alpha) \sim e^{\alpha W[C]}\,, \quad \psi_1 \sim \left(W[C] - \frac{I_2(2\alpha)}{I_1(2\alpha)} \right) \psi_0(\alpha)$$

- Energy Spectrum: Agreement with exact diagonalization across weak and strong coupling limits.
- Energy Gap: Variational results match the expected gap $\Delta E \sim 2\sqrt{\lambda}$ for large λ.

Two plaquettes

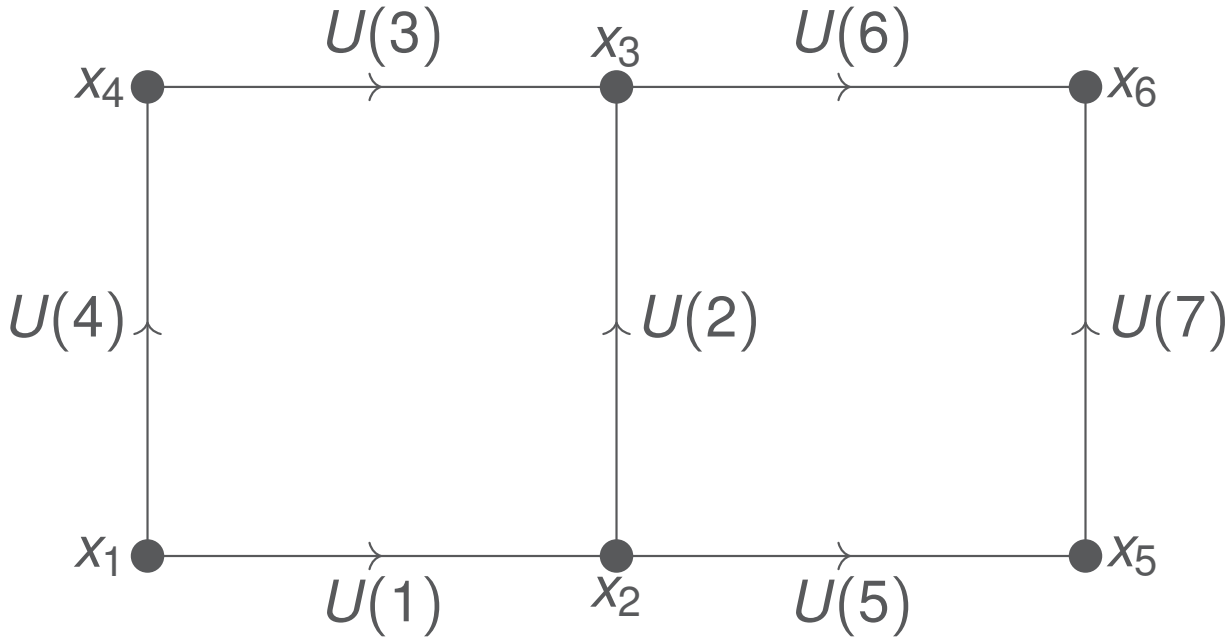

2 independent d.o.f.:

$$X(1) = U(4)U(3)U(2)^\dagger U(1)^\dagger \ , \quad X(2) = U(1)U(5)U(7)U(6)^\dagger U(2)^\dagger U(1)^\dagger$$

Hamiltonian:

$$H_E = \frac{1}{2}\Big([\vec{L}(1)]^2 + [\vec{K}(1)]^2 + 2[\vec{L}(2)]^2 + [\vec{K}(2)]^2 + \frac{1}{2}(\vec{K}(2) + 3\vec{L}(2)) \cdot (\vec{K}(1) - \vec{L}(1))\Big)$$

$$H_M = \lambda(2 - x_0(1) - x_0(2))$$

where $L_i(a) = \frac{1}{2}\epsilon^{ijk} J_{jk}(a)$, $K_i(a) = J_{0i}(a)$.

Results for 2 plaquettes

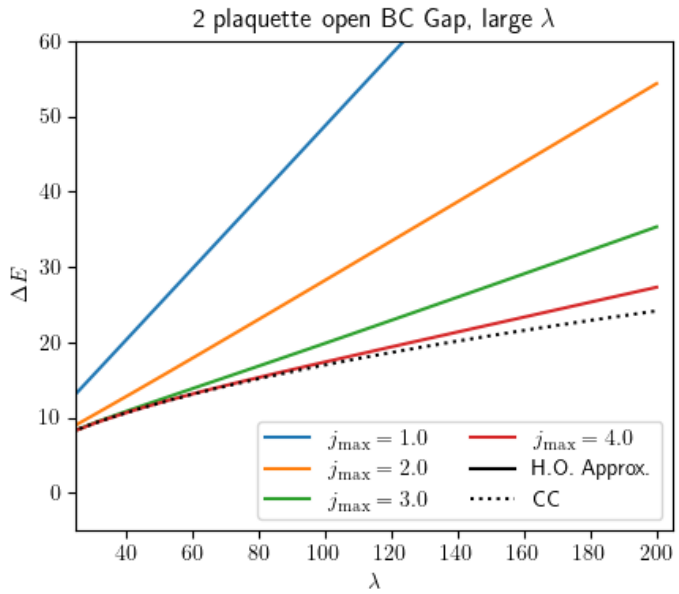

Trial wavefunctions :

$$\psi_0(\alpha) \sim e^{\alpha(W[C_1]+W[C_2])}, \quad \psi_1 \sim \left(W[C_1 \cup C_2] - \left(\frac{I_2(2\alpha)}{I_1(2\alpha)} \right)^2 \right) \psi_0(\alpha)$$

Energy Gap: Variational results $\Delta E = 1.75\sqrt{\lambda}$ close to the expected gap $\Delta E \sim \sqrt{3\lambda}$ for large λ.

Ladder of Plaquettes

Chain of N plaquettes with open boundary conditions.

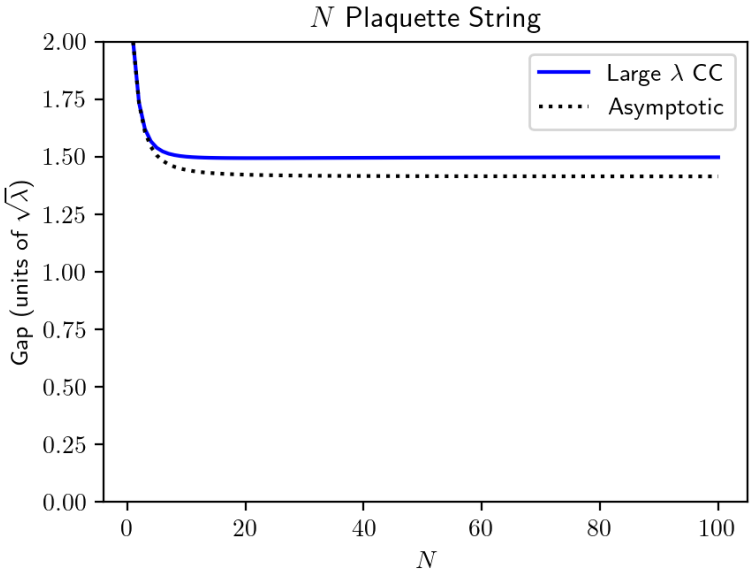

- Hamiltonian: Coupled angular momentum operators across links.
- Gauge Fixing: Maximal tree gauge reducing redundant degrees of freedom.
- Energy gap matches exact $\Delta E \sim 2\sqrt{\lambda}\sqrt{1-\frac{1}{2}\cos\frac{\pi}{N+1}}$ to within 6%.

2D Plaquette Grid

A square lattice of $(N+1) \times (N+1)$ sites contains N^2 plaquettes and a total of $2N(N+1)$ gauge links.

- After using Gauss's law at all but one site, we fix $(N+2)N$ links, leaving N^2 physical links matching the number of plaquettes.
- Gauss's law at the remaining site further restricts physical states to the states of zero total angular momentum.

For large λ, the mass gap is

$$\Delta E_{N\times N} = 2\sqrt{2\lambda}\sin\frac{\pi}{2(N+1)} + \mathcal{O}(\lambda^0)\,.$$

The gap vanishes in the large volume limit ($N \to \infty$) in the strict $\lambda \to \infty$ limit.

- However, the gap is finite as $N \to \infty$, if we include next-to-leading-order corrections in $1/\lambda$.

Results for 2D Plaquette Grid

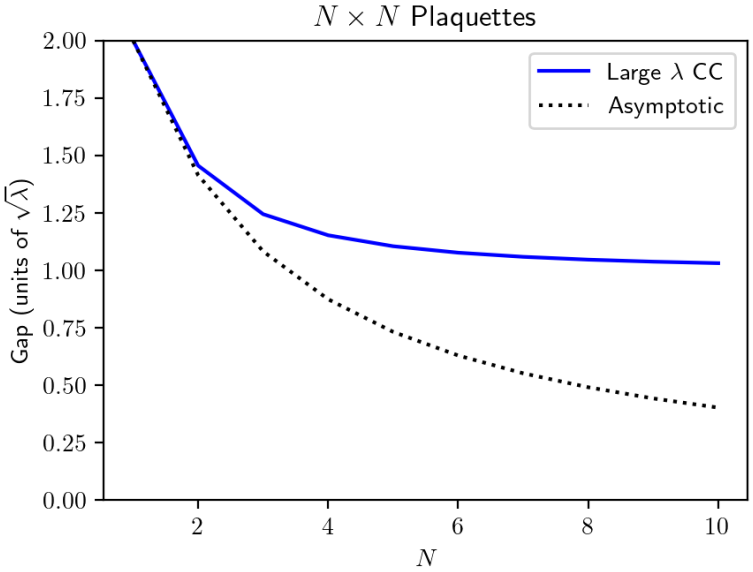

Coupled Cluster Ansatz:

$$\psi_0(\alpha) \propto e^{\alpha \sum_a x_0(a)}\ , \quad \psi_1 \propto \left(\sum_{a,b} A_{ab} \boldsymbol{x}(a) \cdot \boldsymbol{x}(b) - \beta \right) \psi_0(\alpha)$$

with A_{ab}, β appropriately defined.

- Energy gap for large λ, $\Delta E_{N\times N} \sim \left(1 + 2\sin^2 \frac{\pi}{2(N+1)}\right) \sqrt{\lambda}$.
- Need better CC Ansatz, $\psi_0(\alpha) \propto e^{\alpha\left(\sum_a x_0(a) + \sum_{ab} B_{ab} \boldsymbol{x}(a)\cdot\boldsymbol{x}(b)\right)}$

Quantum Simulation with Qumodes

Algorithm: Represent SU(2) links using four qumodes per link.
Advantages:

- Direct representation of angular momentum algebra.
- Efficient implementation of Wilson loop operators.

We introduce a quadruplet of qumodes with quadratures $\boldsymbol{q} = (q_0, q_1, q_2, q_3)$ and $\boldsymbol{p} = (p_0, p_1, p_2, p_3)$, obeying the commutation rules $[q_\mu, p_\nu] = i\delta_{\mu\nu}$ $(\mu, \nu = 0, 1, 2, 3)$. They take values on the entire real axis.

- To restrict them, we consider wave functions $\psi(\boldsymbol{q})$, which only have support close to the unit sphere ($\boldsymbol{q}^2 \approx 1$).
- We impose this constraint by including a factor of the form

$$e^{-\frac{\Lambda^2}{2}(\boldsymbol{q}^2-1)^2},$$

- reduces to a Dirac δ-function $\delta(\boldsymbol{q}^2 - 1)$ in the limit $\Lambda \to \infty$.

Coupled Cluster Ansatz

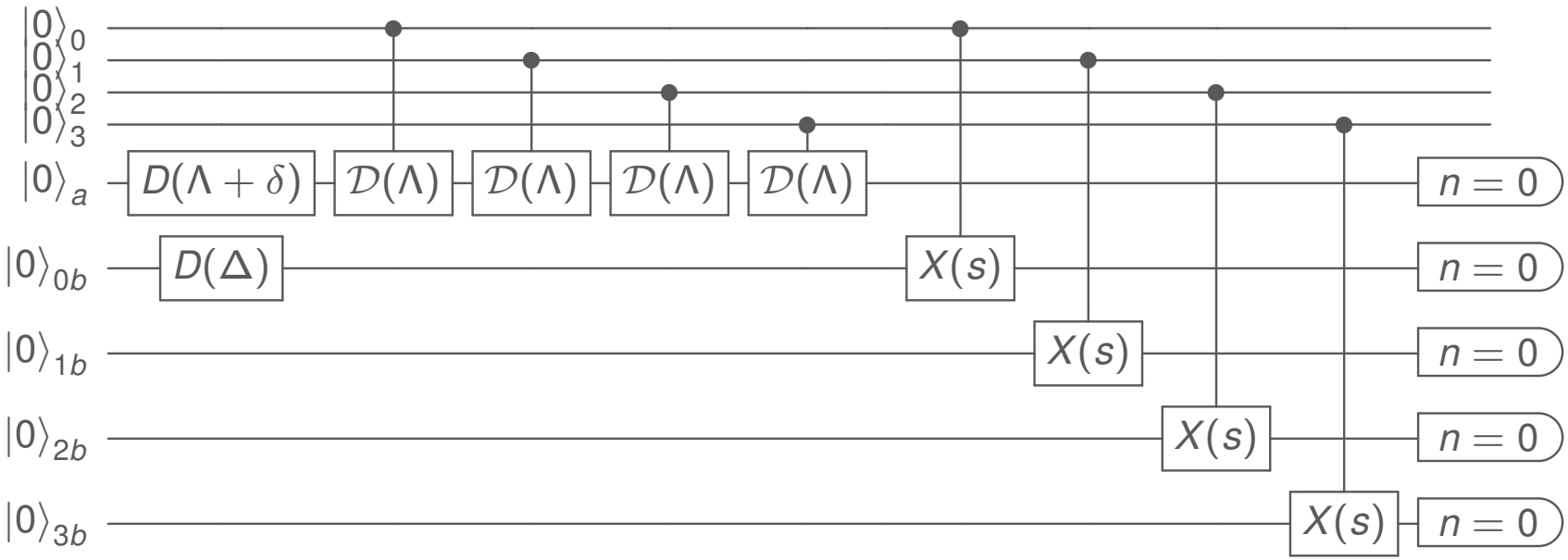

Quantum circuit that generates the CC ground state Ansatz

$$\psi_0^{QC}(\alpha;\boldsymbol{q}) = e^{\alpha q_0}\ e^{-\frac{\Lambda^2}{2}(\boldsymbol{q}^2-1)^2}$$

with adjustable parameter s, $\delta = \frac{1+s^2}{2\Lambda}$, and $\Delta = \frac{\alpha}{s}$.
First excited state:

$$|\psi_1^{\mathrm{QC}}(\alpha)\rangle \propto (q_0-\beta)\,|\psi_0^{\mathrm{QC}}(\alpha)\rangle\ , \qquad \beta = \frac{I_2(2\alpha)}{I_1(2\alpha)} + \frac{\alpha}{4\Lambda^2} + \mathcal{O}(\frac{1}{\Lambda^4})$$

Quantum Simulation Results

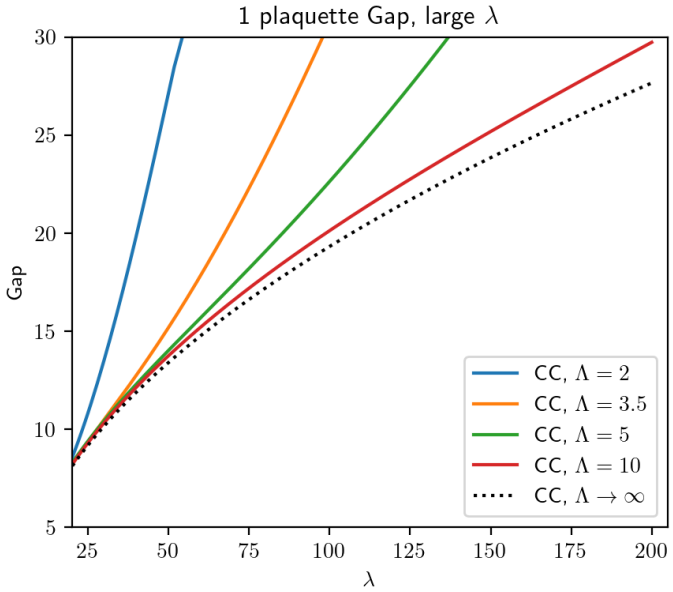

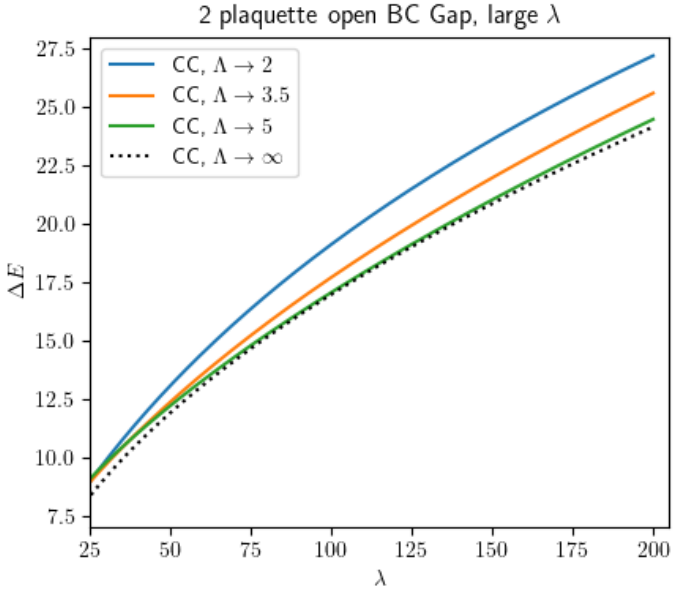

Energy gap of one (left) and two (right) plaquettes.

Hamiltonian for 1 plaquette:

$$H^{\mathrm{QC}} = \frac{1}{2}(\vec{L}^2 + \vec{K}^2) + \lambda(1 - q_0)\ ,\ \vec{L} = \vec{q} \times \vec{p}\ ,\ \vec{K} = \vec{q}p_0 - q_0\vec{p}$$

For 2 plaquettes:

$$H^{\mathrm{QC}} = \frac{1}{2}\Big([\vec{L}(1)]^2 + [\vec{K}(1)]^2 + 2[\vec{L}(2)]^2 + [\vec{K}(2)]^2 + \frac{1}{2}(\vec{K}(2) + 3\vec{L}(2)) \cdot (\vec{K}(1) - \vec{L}(1))\Big)$$

$$+\lambda(2 - q_0(1) - q_0(2))$$

N Plaquettes

A system on a lattice with N plaquettes can be simulated with N qumode quadruplets of quadratures $(\boldsymbol{q}(a), \boldsymbol{p}(a))$ $(a = 1, 2, \ldots, N)$. N grows linearly with the volume. Hamiltonian:

$$H^{\mathrm{QC}} = \frac{1}{2} \sum h^{\mu\nu\rho\sigma}(a,b) J_{\mu\nu}(a) J_{\rho\sigma}(b) + \lambda \left[N - \sum_a q_0(a) \right] ,$$

Trial states

$$|\varphi_0^{\mathrm{QC}}(\alpha)\rangle \propto e^{\alpha \sum_{ab} B_{ab} \boldsymbol{q}(a)\cdot\boldsymbol{q}(b)} |\psi_0^{\mathrm{QC}}(\alpha)\rangle$$

$$|\varphi_1^{\mathrm{QC}}(\alpha)\rangle \propto \left(\sum_{a,b} A_{ab} \boldsymbol{q}(a) \cdot \boldsymbol{q}(b) - \beta \right) |\varphi_0^{\mathrm{QC}}(\alpha)\rangle$$

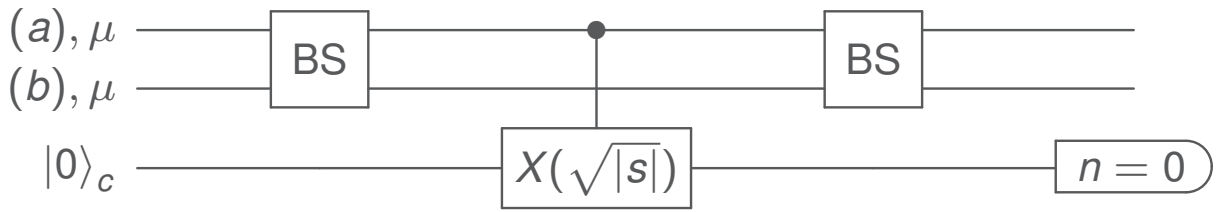

Quantum circuit that generates a factor of the form $e^{-\frac{|s|}{2}(q_\mu(a)+q_\mu(b))^2}$, required for the trial states.

Time evolution

After Trotterization, each term contributing to the Hamiltonian can be implemented independently for small time intervals.

- For the magnetic part, we need to implement Gaussian displacement operators, $e^{i\lambda\Delta t q_0(a)}$, a total of N gates.
- Terms in the electric part are of the form $e^{-isJ_{\mu\nu}(a)J_{\rho\sigma}(b)}$, and can be implemented with:

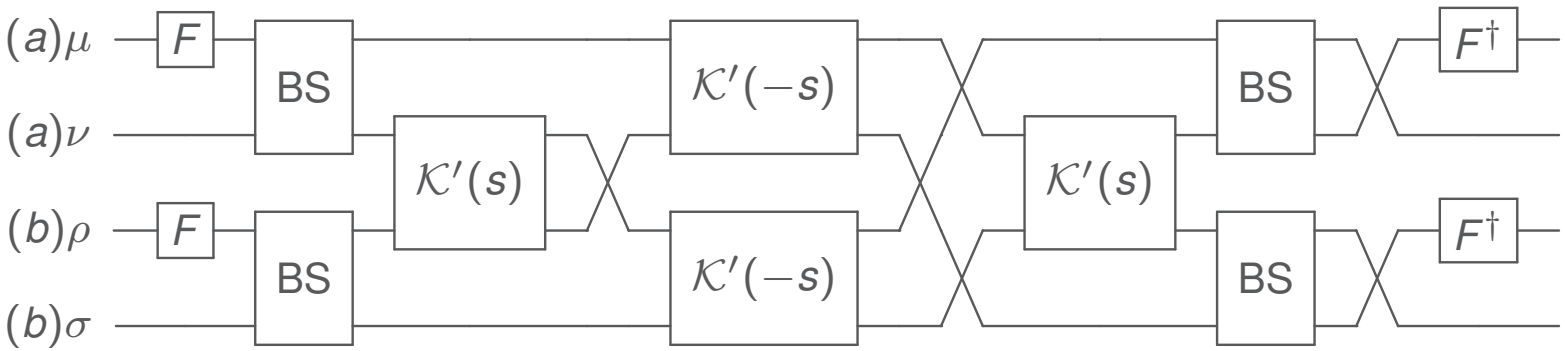

Cross-Kerr gate $\mathcal{K}'_{\mu\nu}(s) = e^{isN_\mu N_\nu}$, $N_\mu = \frac{1}{2}(p_\mu^2 + q_\mu^2)$.

We need $\mathcal{O}(N^2)$ quantum resources to implement them.

Conclusion

There are significant experimental advantages in using CV systems, mainly realized with photons, for quantum information processing. Algorithms based on CV rival their DV counterparts in efficiency, and can be implemented with current technologies.

Path to QCD:

- Introduce fermionic fields – non-trivial due to the doubling problem – use Wilson fermions, or staggered fermions, or domain wall fermions. Better with DV (qubits)? Explore QC that combines qubits (quarks) with qumodes (gluons).
- Address renormalization on the lattice, including non-perturbative renormalization techniques.
- Extend lattice QCD calculations to finite temperature and finite baryon density, exploring the QCD phase diagram.
- Explore and develop new algorithms and computational techniques, such as machine learning methods, to further enhance the efficiency and accuracy of lattice QCD quantum simulations.

Questions and Discussion

Thank you!